



Published in final edited form as:

Gene Ther. 2014 January ; 21(1): 71–80. doi:10.1038/gt.2013.59.

Virally-expressed connexin26 restores gap junction function in the cochlea of conditional *Gjb2* knockout mice

Qing Yu^{1,3,#}, Yunfeng Wang^{2,#}, Qing Chang³, Jianjun Wang³, Shushen Gong¹, Huawei Li², and Xi Lin³

¹Department of Otolaryngology Head & Neck Surgery, Beijing Tongren Hospital, Capital Medical University, #1 Dong Jiao Min Xiang Street, Beijing, China 100730

²Department of Otolaryngology, Eye & ENT Hospital, Shanghai, Fudan University, Shanghai, China 200031

³Department of Otolaryngology, Emory University School of Medicine, 615 Michael Street, Atlanta, GA 30322-3030, USA

Abstract

Mutations in *GJB2*, which codes for the gap junction protein connexin26, are the most common causes of human nonsyndromic hereditary deafness. We inoculated modified adeno-associated viral vectors into the scala media of early postnatal conditional *Gjb2* knockout mice to drive exogenous connexin26 expression. We found extensive virally-expressed connexin26 in cells lining the scala media, and intercellular gap junction network was re-established in the organ of Corti of mutant mouse cochlea. Widespread ectopic connexin26 expression neither formed ectopic gap junctions nor affected normal hearing thresholds in wild type mice, suggesting that autonomous cellular mechanisms regulate proper membrane trafficking of exogenously-expressed connexin26 and govern the functional manifestation of them. Functional recovery of gap-junction-mediated coupling among the supporting cells was observed. We found that both cell death in the organ of Corti and degeneration of spiral ganglion neurons in the cochlea of mutant mice were substantially reduced, although auditory brainstem responses did not show significant hearing improvement. This is the first report demonstrating that virally-mediated gene therapy restored extensive gap junction intercellular network among cochlear non-sensory cells *in vivo*. Such a treatment performed at early postnatal stages resulted in a partial rescue of disease phenotypes in the cochlea of the mutant mice.

Keywords

Gjb2; scala media; cochlea; gene therapy; connexin26; hearing; deafness

Users may view, print, copy, download and text and data- mine the content in such documents, for the purposes of academic research, subject always to the full Conditions of use: http://www.nature.com/authors/editorial_policies/license.html#terms

*Correspondence should be addressed to Xi Lin, PhD, Department of Otolaryngology, Emory University School of Medicine, 615 Michael Street, Whitehead Building #543, Atlanta, GA 30322. Telephone: 404-727-3723, Fax: 404-727-6256, address: xlin2@emory.edu.

#equal contribution authors

Conflict of interest: Authors declare no conflict of interest in this study.

Supplementary information is available at GT's website.

Introduction

Genetic mutations are responsible for about half of all congenital hearing loss cases, which have a prevalence of about 1-2 in every 1,000 births in humans¹⁻². Genetic studies of hearing loss have identified more than 100 deafness genes and established that monogenic mutations in these genes cause the disease³. Importantly, epidemiological studies have revealed that a large proportion of genetic deafness cases (30-50% among various ethnic groups) is caused by loss-of-function mutations in a single gene, *GJB2*, which codes for a major cochlear gap junction (GJ) protein, connexin26 (Cx26)⁴⁻⁷. GJs generally provide an extensive network which allows for intercellular coupling among non-sensory cells in the mammalian cochlea. However, the molecular mechanisms for deafness caused by *GJB2* mutations are currently unclear. No treatment is available to correct the root cellular and genetic causes of sensorineural hearing loss caused by such mutations. With the availability of Cx26 null mouse models⁸⁻¹⁰, a variety of methods (e.g., gene therapy, stem cell transfer, etc.) may be tested to restore hearing in these mutant mice.

In 2005 limited success in correcting a specific dominant *GJB2* point mutation in a mouse model using a RNA interference approach was reported¹¹. For the more common form of *GJB2* functionally-null mutations, one promising treatment lies in virus-mediated connexin expression to re-establish the extensive GJ intercellular network in affected cochlear cells. Experiments have demonstrated that exogenous reporter genes (e.g., green fluorescent protein (GFP)) are expressed by various types of viral vectors in the inner ear with different transduction efficiencies and cell specificities¹²⁻¹⁶. One recent report using bovine adeno-associated virus vectors shows that *in vitro* treatment could restore Cx26 protein expression and rescue gap junction coupling in cultured cochlear tissues isolated from conditional Cx26 null-mutant mice¹⁷. However, the *in vivo* feasibility of gene therapy in correcting the most common form of human genetic deafness, *GJB2* null mutations, remains to be investigated.

Although a high incidence of human genetic deafness caused by functionally-null mutations in the *GJB2* in many ethnic groups has been recognized for at least fifteen years^{5-6, 18}, no studies have yet investigated the effect of *in vivo* virally-mediated Cx26 expression¹⁵. One prominent disease phenotype in conditional *Gjb2*-null mutation mice is massive cell death in the middle and basal turns of sensory epithelium in the adult organ of Corti. Cells in the apical turn stay in the immature developmental state and the tunnel of Corti never opens in the adult stage¹⁰. Such a pathogenic process suggests that any gene therapy attempts to correct the *Gjb2* defects at the adult stage is unlikely to succeed because native cochlear cells either degenerate or are unable to develop normally. In contrast, morphological development of the cochlea appears to be normal in cCx26KO mice before the tunnel of Corti starts to open around P9¹⁰, which suggests a potential window of opportunity for treatment before the cells die in the sensory epithelium. This motivated us to investigate the effects of virally-mediated exogenous Cx26 expression in early postnatal cochlea. Our results showed extensive expression of Cx26 and re-establishment of the GJ network in various types of cochlear cells lining the scale media. Ectopic cochlear Cx26 expression did not affect normal hearing in WT mice. We achieved both high transduction efficiency among various cochlear non-sensory cells and preservation of normal hearing sensitivity

after direct inoculation of AAV into the scala media, thus solving two critical issues in treating *Gjb2* related deafness by the gene therapy approach in mouse models. Functional tests revealed that such a gene therapy approach considerably corrected or improved many aspects of the disease phenotypes in the cochlea of cCx26KO mice, although the hearing sensitivity was not restored in these mutant mice.

Results

Viral inoculation into the scala media resulted in extensive exogenous Cx26 expression and formation of GJs

Cochlear GJs form an extensive intercellular network connecting all types of non-sensory cells in the sensory epithelium, lateral wall and spiral limbus¹⁹⁻²⁰. In order to re-establish the cochlear GJs as extensively as possible in those cells in the cCx26KO mice, we inoculated viruses directly into the scala media since such an approach was able to achieve much better viral transduction in cochlear cells lining the scala media compared to other injection routes, such as injections made into the scala tympani through the round window (RW) (Fig. S1). The results are consistent with published studies by others^{12-13, 15-16, 21}. By injecting viral vectors into early postnatal (P0-P1) scala media, we avoided causing any hair cell loss at the site of injection or at any other cochlear sites¹⁶. More importantly, ABR tests made one month later showed that hearing thresholds from 4k to 32 kHz were not affected in WT mice (filled reverse triangle, Fig. 7). We used contralateral un-injected cochlea from the same mice as controls (Figs. 2-6). No fluorescent GFP signal was ever observed from the control cochleae or in the spiral ganglion neurons, which suggested that the viral vectors only inoculated cells locally in the enclosed endolymphatic space. Fig. 1 compares Cx26 expression in a WT cochlea (Fig. 1A, obtained by immunolabeling of Cx26) and in the cochlea of cCx26KO mice (Fig. 1B). We distinguished the exogenous Cx26 from endogenous Cx26 by immunolabeling the tagged fusion GFP, since conditional *Gjb2* gene deletions may not be 100% complete in the cochlea of cCx26KO mice¹⁰. Observing from the surface view of a large region of cochlear cells, as made possible on a flattened cochlear preparation²², we found virally-mediated Cx26 expression in many types of cochlear cells (Fig. 1B & Fig. 2, G-I). The viral transduction efficiency tends to be highest in the basal turn, which may be explained by a viral titer gradient created here, as we always injected a small volume (0.2-0.5 μ l) into the basal turn. The details about the transduction efficiencies in various types of cochlear cells at different cochlear turns are given in Table1. Outer sulcus cells had the highest transfection rate of all types of cochlear cells which was nearly 100% at all the cochlear turn, followed by the spindle-shaped cells in the stria vascularis. Ectopic expression in the marginal and spindle-shaped cells was significant, which ranged from 20-60%. The lowest transfection rate (11-13%) was found in the hair cells and outer sulcus cells at the apical turn.

Virally-mediated Cx26 expression was found in cells where Cx26 is normally expressed, and ectopically in the hair cells, spindle-shaped cells and marginal cells in the stria vascularis (compare Fig. 1, A&B). Enlarged views are presented in Fig. 2 for detailed comparisons. Cochlear GJs were re-established extensively in almost all Claudius cells (compare Fig. 2, A, D&G) and outer sulcus cells (compare Fig. 2, B, E&H) in the cochlea of

cCx26KO mice after injection with the viral construct (Fig. 2, G&H). Nearly all outer sulcus cells appeared to be connected by re-established GJs. In the Claudius cells, however, it seemed that GJs in the cell membrane tended to form in cells whose neighboring cells were all transfected and expressed Cx26. One example is indicated by an arrowhead in Fig. 2G. When Cx26 expression in some of the surrounding cells were below the detection level or some of the surrounding cells were not transfected, we found that the Cx26 protein in those cells tended to stay in the intracellular space and few GJ-plaque-like immunostaining was seen in the membrane of outer sulcus cells. Examples are pointed out by small arrows in Fig. 2G. The non-disrupted immunolabeling pattern in the membrane of Claudius cells, which correlate with the size of GJ plaques²³, appeared to be smaller in virally-expressed cochlea as well (compare Fig. 2, A&G, B&H). We estimated that the re-established GJ plaques were $53\pm 11\%$ (N=62) and $36\pm 8.3\%$ (N=78) the size of WT plaques in Claudius cells and outer sulcus cells, respectively. In addition, we observed that at least one important type of supporting cells, the Hensen's cells, expressed Cx26 poorly in our studies (compare Fig. 2, A&G).

In addition to re-established GJs in the cell membrane, strong intracellular Cx26-GFP signal was observed in a large number of marginal cells (ranging from 45-21% in different turns, Table1), spindle-shaped cells (61-32%, Table 1) and hair cells (44-13%, Table1) where Cx26 is not normally expressed in WT cochlea (comparing Fig. 1 and Fig. 2, C, F&I). We never observed aggregation of GFP signal in the cell membrane and formation of GJ-like plaques in the membrane of these cells (Fig. 1B & Fig. 2I). Differential trafficking and targeting pattern of Cx26 in various epithelial cell types suggest that targeting and clustering of Cx26 might depend on other factors that are specifically expressed in only a subset of epithelial cells in the cochlear supporting cells. Such regulatory mechanisms should play a critical role in cochlear functions as the ectopic Cx26 expression didn't result in the formation of GJs in these cochlear cells, and normal hearing thresholds in WT mice was not affected (Fig. 7, curve with reverse triangle data points).

Re-established cochlear GJs partially restored intercellular coupling in the cochlea of cCx26 KO mice

We used two independent methods to test whether the re-established GJs recovered intercellular coupling in the cochlea of cCx26KO mice. GJ-mediated intercellular coupling among the supporting cells was first tested by dye diffusion assay, in which a charged fluorescent dye (propidium iodide, PI) was injected intracellularly into the outer sulcus cells and its diffusion over a period of time across GJs to neighboring cells was observed. Fig. 3 compares the time course of dye diffusion in the outer sulcus cells of WT mice (Fig. 3A, image panels presented in the bottom row), virus-injected cCx26KO mice (Fig. 3A, image panels given in the middle row) and cCx26KO mice without injections (Fig. 3A, image panels in the top row). In Fig. 3B, exogenous GJ plaques in the cell membrane providing intercellular coupling were visualized by the green GFP among these cells. Comparison of the dye diffusion results showed partial but considerable functional recovery in the cochlea of mice that received virus injections. The quantification results (Fig. 3C) showed that a significant amount of intercellular coupling, as measured by the number of cells which received GJ-mediated dye diffusion from the injected cell over time, was significantly

restored among the cells which received virus injections, although there was still a substantial difference comparing to the WT cells. Another independent method we used to evaluate the amount of intercellular GJ-mediated coupling was the fluorescence recovery after photo-bleaching (FRAP) assay. Photobleached cells are indicated by small arrows in Fig. 4A. A series of images taken around the time when the cells were photobleached are given in the top, middle and bottom rows for WT, virus injected mutant mice and cCx26KO mice without injection, respectively (Fig. 4A). We measured the intensity of fluorescence recovery over time for the cell indicated by arrows (Fig. 4A). The recovery results from photobleaching were normalized as the percentage of baseline fluorescence before photobleaching was given (Fig. 4B, n=10). The results showed that the average time to reach the half intensity of steady-state recovery was 0.47 ± 0.03 , and 2.3 ± 0.4 for WT and virus inoculated outer sulcus cells, respectively. The same cells in the cCx26KO showed no recovery at all.

Functional improvement in the injected cochleae of cCx26Ko mice was supported by the observation that there was a considerable lessening of morphological abnormality and a notable prevention of SG neuron degeneration in the cochlea of the mutant mice that received virus injections. Fig. 5 compares the morphology of the organ of Corti in WT mice (Fig. 5A, image panels a-c in the left column), cCx26KO mice with virus injection (Fig. 5A, image panels g-i in the right column) and cCx26KO mice without virus injection (Fig. 5A, image panels d-f in the middle column). Cell death in the middle and basal turns was substantially reduced (compare Fig. 5A, panels e&h). The tunnel of Corti (indicated by arrows in Fig. 5A, h&i) was partially opened in the treated cochleae in the middle (compare Fig. 5A, panels e&h) and basal (compare Fig. 5A, panels f&i) turns, although the opening was not as wide as the WT organ of Corti (panels a-c), and the tunnel of Corti remained closed in the apical turn (indicated by an arrow in the Fig. 5g). In our published papers we have described that the cellular degeneration started in the middle turn, then spread to the basal turn in the cochlea of cCx26 KO mice with a variable time course^{10, 21}, resulting in variation of cell death in the basal turn among individual animals. With the inoculation of virus, we generally observed that death of hair cells was significantly reduced in the middle and basal turns. The hair cells in the organ of Corti were counted in the whole-mount cochlear preparation (Fig. 5B). Although the difference among apical hair cells were small between the treated (51.8 ± 2 per 100 μm linear length) and untreated sides (53.1 ± 1 per 100 μm linear length), the effect was more significant in the middle and basal turns. There was a substantial difference in the survival of hair cells between the treat (40.0 ± 4.4 per 100 μm linear length) and untreated (1.9 ± 0.4 per 100 μm linear length) cochleae in the middle turn (Fig. 5B, comparing two panels in the middle column). In the basal turn the survived hair cells increased from 25.0 ± 4.3 per 100 μm linear length in the untreated side to 43.8 ± 4.1 per 100 μm linear length as a result of viral-mediated Cx26 expression (Fig. 5B, comparing two panels in the right column).

No transfection of SG neurons was observed after viral inoculation. Better cell survival in the organ of Corti, however, apparently prevented secondary death of SG neurons. Fig. 6A compares SG neuron degeneration in the apical, middle and basal turns of the treated and untreated cochlea. Quantification (given in Fig. 6B, with SG neuron density normalized to the results obtained from WT cochlea) of the survival of SG neurons showed that virally-

mediated Cx26 expression substantially increased SG neuron survival in the middle and basal turns. The apical SG neurons in cCx26KO mice were relatively intact²¹, therefore the effect of viral treatment on promoting survival of these neurons was not significant. It is interesting to note that in WT mice the density of SG neurons in middle turn was higher than that in the basal turn (Fig. 6B), which is consistent with our published results²¹. Fig. 7 shows the results of frequency-specific ABR tests measured by tone-burst, in which the hearing thresholds of four groups of mice were tested. Similar thresholds were obtained in WT mice (n=8, data shown with hollow reverse triangles) and WT mice which received virus injections (n=8, data shown with filled reverse triangles), indicating that our surgical procedures and the virally-mediated Cx26 expression did not damage hearing. The hearing of cCx26KO mice, in the ears which received viral injection (n=8, data points with hollow circles) and the untreated contralateral side (n=8, data points with filled circles), both showed substantial threshold elevations compared to WT mice. The thresholds of the treated and untreated ears showed no statistical differences at frequencies ranging from 4 kHz to 32 kHz. Our conclusion is that partial morphology recovery in treated cCx26KO mice apparently was not enough to bring back hearing sensitivity.

Discussion

One of the major difficulties in successfully treating disease phenotypes caused by *GJB2* null mutations with a gene therapy approach is the apparent requirement of wide-spectrum expression of exogenous *GJB2* in all types of non-sensory cells, since it is known that cochlear gap junctions connect all cells except the hair cells in the cochlea of WT mice^{21, 24}. We have employed a number of novel approaches in this study in order for virally-mediated Cx26 expression to be as extensive as possible in the cochlear cells. Our first series of experiments found that injections made into the scala tympani through the round window resulted in little Cx26 expression in cells lining the scala media (Fig. S1). This result was consistent with most previous reports^{12-13, 15-16}. We therefore performed a localized virus-mediated gene transfer directly into the small volume of the scala media of early postnatal (P0-P1) mice, as our published results showed that this approach is likely the most appropriate for preserving the hearing sensitivity¹⁶. Such a treatment also maximizes the efficiency for virus to access all types of cochlear cells lining the scala media and minimizes possible side effects of gene therapy by reducing the chance of general adverse general immuno-effects or other genetic complications. Large numbers of gene therapy studies aiming for hearing rescue have been conducted in the cochlea¹²⁻¹⁶. The focus of past studies, however, has mostly been on regenerating sensory cells from survived supporting cells or by using a cell replacement approach to restore normal inner ear functions¹⁵. Transforming survived cells into hair cells is unlikely to successfully treat deaf patients suffering from genetic mutations because the causative mutation still remains in the genome. The new hair cells, even if successfully regenerated, will still suffer consequences of the original genetic mutation. An effective approach is gene-based therapy for treating genetic deafness which consists of introducing exogenous expression of normal copies of the mutated gene in affected cells. Most studies^{14, 25-27} have shown that injections made directly into the scala media in adult animals produce side-effects such as the breaking of cochlear structure, mixing of the perilymph and endolymph, all of which invariably lead to

severe hearing loss^{14, 28-29}. In this study we demonstrated that transgene expression with our approach of injecting into the cochlea of early postnatal mice was localized within the scala media, with minimal leak to the scala tympani, and no spread to surrounding tissue and contralateral cochlea. Our follow-up studies showed functional recovery of the cochlear GJ network (Figs. 3&4) as well as important phenotypic improvement of the injected cochlea, as compared to the contralateral non-injected cochlea (Figs. 5&6). In addition to these novel findings, we demonstrated for the first time that extensive ectopic Cx26 expression in cochlear cells of WT mice did not affect normal hearing (Fig. 7). Interestingly, our previous study also showed that high levels of GFP expression in a large number of cochlear cells did not harm hearing sensitivity¹⁶. These results validated our surgical procedures and demonstrated that excess virally-expressed exogenous protein is not necessarily harmful to cochlear function. These results are encouraging for future gene therapy for the treatment of *GJB2* mutations since ectopic gene expression is usually unavoidable after viral vectors are inoculated into tissue.

Many viral vectors have been tested for *in vivo* expression of exogenous genes in the cochlea, including adenovirus¹², Adeno-associated virus (AAV)³⁰, lentivirus^{27, 31}, herpes simplex type I virus, vaccinia virus¹³, and bovine Adeno-associated virus¹⁴. Our previous observations suggested that AAV2/1 injected before postnatal day 5 yielded the best results in terms of achieving the most widespread exogenous expression of GFP in the inner ear of mice. Another potential advantage of AAV-mediated transgene transfer is that its expression has been shown to last for several months³². When compared to results reported by a recently-published paper³³ in which congenital deaf mice lacking the vesicular glutamate transporter-3 (*VGLUT3*) were successfully treated, we noticed a few important similarities as well as differences. First, we observed that the exogenous Cx26 protein was expressed in both the targeted cells and ectopically in many other types of cochlear cells, whereas virally-expressed *VGLUT3* protein was only detected in the intended targeted cells (the inner hair cells). Despite ectopic Cx26 expression, cell autonomous regulatory mechanisms governing protein trafficking and assembly of GJ plaques apparently restricted the formation of functional GJs only among those cells that are normally coupled by GJs in WT mice. It seemed that both virally-expressed *GJB2* and *VGLUT3* were only functionally manifested in their intended targets. Secondly, we were able to achieve a nearly 100% Cx26 expression in the outer sulcus cells. However, the transduction efficiency for other types of cochlear cells was not as complete, especially in the Hensen's cells (Table 1). In comparison, the *VGLUT3* is expressed in 100% of inner hair cells³³ even when viruses were injected to the scala tympani, from which hair cells are separated by the tightly sealed basilar membrane. The reason for these disparities is not clear and certainly warrant future studies, although one might speculate that the difference may be due to the unique post-transcriptional regulation of the *VGLUT3* gene or virus titer differences.

Our initial motivation for this study was to answer the following questions: (1) What is the extent and specificity of virally-mediated *Gjb2* expression in the cells lining the scala media if we directly inoculate viral vectors into the endolymphatic space? Will the surgical procedure for viral inoculation itself damage hearing sensitivity? (2) Will the exogenous Cx26 protein be properly transported to the cell membrane and form functional GJs? What

are the functional consequences of ectopically expressed Cx26 in the cochlea? (3) What disease phenotypes caused by *Gjb2* null mutation in the mouse model can be corrected by our gene therapy treatment? Our results provided answers to most of these questions. We showed for the first time that restoration of the extensive gap junction intercellular network among cochlear non-sensory cells *in vivo* is possible by a virally-mediated gene therapy approach in cCx26KO mice. Partial morphological rescue of the cells in the organ of Corti, especially in the middle and basal turns, and the prevention of degeneration of the SG neurons provided evidence of important treatment effect of gene therapy. The reason for little improvement in hearing thresholds of cCx26KO mice is currently unknown and can only be speculated upon here for future studies. We injected viral vectors at P0-P1 into the scala media, but AAV-mediated exogenous gene expression takes about one week to reach the maximal stable level¹⁶. It is possible that we missed the critical window for rescue when Cx26 is uniquely required for the development of the organ of Corti³⁴. The percentage of non-sensory cochlear cells transduced by viral vectors certainly needs to be improved, especially in the Hensen's cells (Table 1) in order to form a complete loop of intercellular GJ network in the cochlea. In order to achieve this goal, we may need to inject viral vectors at earlier stages, possibly into the otocyst of embryonic mice since it has been reported that a high transduction rate was obtained after *in utero* delivery to the developing mouse otocyst³⁵⁻³⁶. Recent successful hearing restoration in connexin30 knockout mice achieved by gene therapy treatment delivered at embryonic stage is encouraging³⁷. Alternatively we may need to mix multiple types of virus for the viral delivery in order to improve transduction efficiency since different serotypes of virus may target different types of cochlear cells with different optimal efficiencies¹⁵. In summary, our work represents the first step in investigations on treatment for the most common form of inherited deafness, which is caused by *GJB2* null mutations. We have identified a viral vector (AAV2/1) that targets many types of cochlear cells lining the scala media. Although the transfection rate in many types of cochlear cells and cochlear regions was more than 50%, it is unclear whether or not this percentage of expression is sufficient to restore functional recovery of the cell-cell gap junction network. Nevertheless, our results support the principle of using a virally-mediated gene therapy approach to restore the extensive gap junction intercellular network. By preserving hearing sensitivity and achieving high efficiency exogenous expression of *GJB2* in the inner ear, we have accomplished an important and necessary step in the treatment of congenital deafness cases which require early intervention in order to restore hearing sensitivity. Future investigations are still needed to improve the transduction efficacy of various types of cochlear non-sensory cells, to investigate long-term safety, and to study ethical implications before a gene therapy approach for human congenital deafness disease can become a reality.

Materials and methods

Animal use and surgical procedures for injecting virus into the scala media

Conditional Cx26 knockout mice (Foxg1-cCx26KO) and their littermate wide type (WT) controls were used in this study. Details about the generation and genotyping of Foxg1-cCx26KO mice were given previously described^{10, 21}. Genetic background of mice was C57BL. Animal use protocols were approved by the institutional animal care and use

committee of Emory University. Extensive viral transduction in the cochlea is required for the success of this project because Cx26 is normally expressed by all types of cochlear non-sensory cells¹⁹. However, current surgical procedures used in cochlear gene therapy for microinjections into the scala media usually are performed with adult animals. The procedure severely damage hearing sensitivity¹²⁻¹⁴, thus defeating the purpose of treatment. We recently developed a new injection approach which used early postnatal mice. Such a new procedure avoided damaging mouse hearing sensitivity when mice grow to adulthood¹⁶. With our new method, hearing threshold is preserved if injections into the scala media are done to mice younger than P5. In this study we used P0 (the day mice were born) or P1-old mice for virus injections in order to avoid adversely affect the hearing sensitivity. The results confirmed that injections made into the scala media achieved much better viral transduction in cochlear cells lining the scala media than with injections made into the scala tympani through the round window (RW) (Fig. S1). This finding was also consistent with results obtained by most previous reports^{12-13, 15}.

Injections of 0.2-0.5 μ l of virus-containing phosphate-buffered solution (PBS) were carried out with a Picospritzer III pressure microinjection system (Picospritzer III, Parker Hannifin Corp, NY). Direct monitoring of fluid ejection was made possible by including a fast green dye (Sigma-Aldrich Inc., St Louis) in the solution, which made the movement of fluid ejection out of the pipette visible when observed with a dissection microscope (Zeiss Stemi 2000, Zeiss, Germany) under bright light illumination. For each animal only one side of the cochlea was injected near the basal turn, and the contralateral cochlea was used as a control. Most animals (>90%) survived surgeries and we found no signs of inflammation in the middle and inner ears. Both dye diffusion and FRAP assays were used in functional studies (Figs. 3&4) performed with the flattened cochlear preparation made from P8-P10 mice. Cochlear morphology (Fig. 5) was examined using cochlear specimens obtained from P30-60 mice. We used one-month old mice in the auditory brainstem response (ABR) tests (Fig. 7).

Preparation of viral vectors

Our previous studies suggested that the Adeno-associated virus (AAV) serotype 2/1 gives the best transduction for GFP reporter gene expression in cochlear non-sensory cells, and virally-mediated gene expression driven by the CB7 promoter was more stable and widespread in the cochlea compared to that driven by the CMV promoter¹⁶. We therefore used either AAV-CB7-*Gjb2* (AAV modified to express *Gjb2* driven by the CB7 promoter, titer: 1.5×10^{13} genome copies per ml (GC/ml)) or AAV-CB7-*Gjb2*-GFP (AAV modified to express *Gjb2*-GFP fusion protein driven by the CB7 promoter, titer: 1.2×10^{12} GC/ml,) in this study. The transgene cassettes in the viral constructs consisted of either CMV or CB7 promoter for driving the expression of *Gjb2* or *Gjb2* fused with the GFP. Details of AAV constructs are described in Fig. S2. Viral vectors were prepared by the HOT strategy, which is helper virus free and uses only two plasmids in the transfection step³⁸. AAV was generated at the Emory virus core facility and details of the virus production were given in our published paper¹⁶. The AAV vectors were purified using the iodixanol gradient centrifugation procedure³⁹. Virus titers were measured by real-time PCR⁴⁰. The virus

aliquots (10 μ l each) were kept at -80°C and one aliquot in PBS was thawed prior to the injection.

Histological processing procedures and data analysis

Both injected and un-injected cochleae were processed and compared in order to evaluate the effects of virally-mediated expression of Cx26. Details of the immunolabeling protocols performed with flattened cochlear preparations were given previously^{22, 41}. Primary polyclonal antibodies against Cx26 (dilution 1:200, catalog# 71-0500, Invitrogen, Carlsbad, CA), GFP (1:200, cat#A11122, lot#1024102, Invitrogen, Carlsbad, CA), or Myo6 (catalog#25-6791, lot#100201, 1:200, Proteus BioSciences, CA) were incubated with the specimen overnight at 4°C . The immunolabeling of the primary antibodies was visualized using a goat anti-rabbit IgG antibody conjugated to Alexa Fluor 488 (1:500 dilution, cat# A11008, lot#1166843, Invitrogen, Carlsbad, CA) or a goat anti-mouse IgG antibody conjugated to Alexa Fluor 568 (1:500, cat#A11061, lot#1180091, Invitrogen, Carlsbad, CA). Counterstaining was used to better visualize cell membranes and hair bundles using phalloidin conjugated to Alexa568 (catalog#P-1951, lot#093K0474, dilution 1:1000, Sigma, MO). All samples were mounted in fluoromount-G antifading solution (catalog#17984-25, Electron Microscopy Science, PA) and images were acquired with a laser-scanning confocal microscope (Zeiss LSM, Carl Zeiss, Germany).

Epoxy resin cochlear sections were made according to our previously-published protocol²¹. Briefly, mouse tissues were fixed by transcardiac perfusion of 4% paraformaldehyde (PFA) dissolved in PBS. Cochleae were dissected out and subsequently perfused via the oval window with a solution of 2% PFA and 2.5% glutaraldehyde in PBS, and kept in it overnight at 4°C . Decalcification was carried out for 72 hours at 4°C in 0.35M EDTA in PBS (pH 7.4). The cochlear samples were then immersed in 2% osmium tetroxide for 2 hours, followed by gradual dehydration in alcohol of increasing grades, then infiltrated and embedded in epoxy resin. Epoxy resin was purchased from Ted Pella Inc. (catalog#18060, Redding, California). Consecutive cochlear resin sections (5 μ m in thickness) were cut along the modiolar axis using a microtome (Microm, model HM 335E, Germany). Cochlear sections were stained with toluidine blue and examined with a light microscope.

The transduction efficiency of virally-mediated gene expression was measured by counting the number of cells that expressed the GFP signal. SG neuron density was calculated as described in our previously published paper²¹ to compare the number of SG neurons in a given volume of tissue in the Rosenthal's canal of P30-P60 old mice. The resin sections were cut in 5 μ m thicknesses and every other section was used to avoid double counting the neurons. To determine the SGN densities we manually counted the number of survived SG neurons in the cochlear turn using Image J software, and then divided the number of SGNs by the cross-sectional area of Rosenthal's canal to obtain density measures. All quantitative analyses were performed in a blind fashion by two independent investigators to ensure a consistency of counting. GraphPad Prism 5 (GraphPad Software Inc., La Jolla, CA) and Origin 7.0 (OriginLab, Northampton, MA) software were used in data analysis. Statistical analyses were performed using the Student t-tests. Data were presented as mean \pm standard error of the mean (SEM). The level of significance was set at $p < 0.05$.

Functional assays for evaluating GJ functions and ABR tests

To perform the dye diffusion assay, flattened cochlear preparations were placed in a recording chamber mounted on an upright microscope (Axioskop2 FX plus, Carl Zeiss, Germany). The use of DIC optics enabled us to directly recognize different cochlear cell types. Propidium iodide (PI, a positively-charged fluorescent dye) was injected into the cytoplasm of a single cell by forming the whole-cell patch-clamp recording mode. Borosilicate glass capillary pipettes (Sutter Instrument Co., Novato, CA) were pulled on a micropipette Puller (P-2000, Sutter Instrument Inc.) and the electrodes were fire-polished (MF-830, Narishige, Japan) before usage. HEPES buffered HBSS solution (H4891, Sigma, St. Louis, MO, USA) was used as the external bathing solution, which contained (in mM): NaCl 137, Na₂HPO₄ 0.2, KCl 5.4, KH₂PO₄ 0.4, MgCl₂ 1, CaCl₂ 1.2, and HEPES 10. Extracellular solution was perfused at a rate of ~1 drop/second.

The pipeline currents were amplified with an Axonpatch 200B amplifier (Axon Instruments, CA) and digitized with a Digidata 1322A interface (Axon Instrument, CA) in order to monitor and verify the formation of the whole-cell recording mode. Pipettes had an access resistance of about 3 M Ω when filled with an internal solution containing (in mM): 120 KCl, 1 MgCl₂, 10 HEPES, 10 EGTA, pH adjusted to 7.2 with KOH. Fluorescent dye (0.75 mM PI, MW=668 Da, charge=+2, catalog# P1304MP, purchased from Invitrogen Inc.) was supplemented in the pipette solution. Images of intercellular dye diffusion at various time points were recorded by a cooled-CCD camera (AxioCam, Carl Zeiss, Germany). The same exposure time was used for samples obtained from WT and mutant mice at all data acquisition time points. Dye recipient cells were visually identified and counted using the same criteria as that used for images of WT and cCx26KO mice. All experiments were carried out at room temperature (20–25°C).

FRAP assay was performed at the Integrated Cellular Imaging Core of the Emory University. We used calcein AM, which is a non-fluorescent and cell permeant compound until it is hydrolyzed by intracellular esterases into the fluorescent anion calcein, after which the only pathway for intercellular dye diffusion is through the GJ network. Flattened cochlear preparations were incubated with 10 μ M calcein AM (MW= 994.87, catalog#C1430, lot#924140, Invitrogen Inc.) for 30 minutes in HBSS. The specimens were then transferred to the stage of the Nikon A1R point scanning confocal microscope. Cells were viewed with a 63 \times oil immersion objective. We delineated a target cell as the region of interest (ROI) to bleach, and also chose proximal unbleached cells as a reference in measurements. Baseline calcein fluorescence was recorded for 1 minute, followed by focal laser exposure (10 seconds) to bleach the intracellular calcein in the ROI. Fluorescence recovery after photobleaching was monitored for up to 10 minutes. The same bleach intensity and acquisition time was used for samples obtained from WT, cCx26KO and virus injected mice. Image sequences were acquired using software developed by the Emory Integrated Cellular Imaging Core. Data were stored on disk and processed offline using the NIS-Elements Viewer (Nikon Instruments Inc., NY, USA) and Origin7.0 software (OriginLab, USA).

ABR is an objective measurement of the hearing threshold based on sound-evoked potentials⁴². We measured hearing by ABR tests one month after the virus injections were

done. Tone burst sound stimuli were presented with a sound tube attached to a high-frequency speaker (Tucker Davis Technologies, Alachua, FL) to one side of the ear. Sound frequencies were adjusted to 4, 8, 12, 18, 24 and 32 kHz in order to test frequency-specific hearing thresholds. Details of the ABR testing methods are given in our published papers ⁴¹. We also monitored the circling behavior, head tilt and swimming ability of the injected mice, three parameters which reflect vestibular function. No signs of vestibular dysfunction resulting from the surgical procedures and virally-mediated gene expression were found.

Supplementary Material

Refer to Web version on PubMed Central for supplementary material.

Acknowledgments

This study was supported by grants to Wang from the National Nature Science Foundation of China (81100721), and to Lin from National Institute on Deafness and other Communication Disorders (RO1 DC006483 and NIDCD 4R33DC010476). Huawei Li also received grant support from the National Science Foundation of China (#30728029 and #81230019) and 973 program (2011CB504506). We thank Ms. Anne Lin for proofreading the final version of the manuscript.

References

1. Sundstrom RA, Van Laer L, Van Camp G, Smith RJ. Autosomal recessive nonsyndromic hearing loss. *Am J Med Genet.* 1999; 89(3):123–9. [PubMed: 10704186]
2. Smith RJ, Bale JF Jr, White KR. Sensorineural hearing loss in children. *Lancet.* 2005; 365(9462): 879–90. [PubMed: 15752533]
3. Dror AA, Avraham KB. Hearing loss: mechanisms revealed by genetics and cell biology. *Annu Rev Genet.* 2009; 43:411–37. [PubMed: 19694516]
4. Denoyelle F, Weil D, Maw MA, Wilcox SA, Lench NJ, Allen-Powell DR, et al. Prelingual deafness: high prevalence of a 30delG mutation in the connexin 26 gene. *Human molecular genetics.* 1997; 6(12):2173–7. [PubMed: 9336442]
5. Morell RJ, Kim HJ, Hood LJ, Goforth L, Friderici K, Fisher R, et al. Mutations in the connexin 26 gene (GJB2) among Ashkenazi Jews with nonsyndromic recessive deafness. *N Engl J Med.* 1998; 339(21):1500–5. [PubMed: 9819448]
6. Denoyelle F, Marlin S, Weil D, Moatti L, Chauvin P, Garabedian EN, et al. Clinical features of the prevalent form of childhood deafness, DFNB1, due to a connexin-26 gene defect: implications for genetic counselling. *Lancet.* 1999; 353(9161):1298–303. [PubMed: 10218527]
7. Yuan Y, You Y, Huang D, Cui J, Wang Y, Wang Q, et al. Comprehensive molecular etiology analysis of nonsyndromic hearing impairment from typical areas in China. *J Transl Med.* 2009; 7:79. [PubMed: 19744334]
8. Cohen-Salmon M, Ott T, Michel V, Hardelin JP, Perfettini I, Eybalin M, et al. Targeted ablation of connexin26 in the inner ear epithelial gap junction network causes hearing impairment and cell death. *Curr Biol.* 2002; 12(13):1106–11. [PubMed: 12121617]
9. Kudo T, Kure S, Ikeda K, Xia AP, Katori Y, Suzuki M, et al. Transgenic expression of a dominant-negative connexin26 causes degeneration of the organ of Corti and non-syndromic deafness. *Human molecular genetics.* 2003; 12(9):995–1004. [PubMed: 12700168]
10. Wang Y, Chang Q, Tang W, Sun Y, Zhou B, Li H, et al. Targeted connexin26 ablation arrests postnatal development of the organ of Corti. *Biochem Biophys Res Commun.* 2009; 385(1):33–7. [PubMed: 19433060]
11. Maeda Y, Fukushima K, Nishizaki K, Smith RJ. In vitro and in vivo suppression of GJB2 expression by RNA interference. *Human molecular genetics.* 2005; 14(12):1641–50. [PubMed: 15857852]

12. Raphael Y, Frisncho JC, Roessler BJ. Adenoviral-mediated gene transfer into guinea pig cochlear cells in vivo. *Neurosci Lett*. 1996; 207(2):137–41. [PubMed: 8731440]
13. Derby ML, Sena-Esteves M, Breakefield XO, Corey DP. Gene transfer into the mammalian inner ear using HSV-1 and vaccinia virus vectors. *Hear Res*. 1999; 134(1-2):1–8. [PubMed: 10452370]
14. Shibata SB, Di Pasquale G, Cortez SR, Chiorini JA, Raphael Y. Gene transfer using bovine adeno-associated virus in the guinea pig cochlea. *Gene Ther*. 2009; 16(8):990–7. [PubMed: 19458651]
15. Sacheli R, Delacroix L, Vandenackerveken P, Nguyen L, Malgrange B. Gene transfer in inner ear cells: a challenging race. *Gene Ther*. 2012
16. Wang, YF.; Sun, Y.; Chang, Q.; Ahmad, S.; Zhou, BF.; Kim, YJ., et al. Early postnatal virus inoculation into the scala media achieved extensive expression of exogenous green fluorescent protein in the inner ear and preserved auditory brainstem response thresholds. *J Gene Medicine*. 2013. <http://onlinelibrary.wiley.com/doi/10.1002/jgm.2701/abstract>
17. Crispino G, Di Pasquale G, Scimemi P, Rodriguez L, Galindo Ramirez F, De Siat RD, et al. BAAV mediated GJB2 gene transfer restores gap junction coupling in cochlear organotypic cultures from deaf Cx26Sox10Cre mice. *PLoS ONE*. 2011; 6(8):e23279. [PubMed: 21876744]
18. Denoyelle F, Lina-Granade G, Plauchu H, Bruzzone R, Chaib H, Levi-Acobas F, et al. Connexin 26 gene linked to a dominant deafness. *Nature*. 1998; 393(6683):319–20. [PubMed: 9620796]
19. Lautermann J, ten Cate WJ, Altenhoff P, Grummer R, Traub O, Frank H, et al. Expression of the gap-junction connexins 26 and 30 in the rat cochlea. *Cell Tissue Res*. 1998; 294(3):415–20. [PubMed: 9799458]
20. Hoang Dinh E, Ahmad S, Chang Q, Tang W, Stong B, Lin X. Diverse deafness mechanisms of connexin mutations revealed by studies using in vitro approaches and mouse models. *Brain Res*. 2009
21. Sun Y, Tang W, Chang Q, Wang YF, Kong YY, Lin X. Connexin30 null and conditional connexin26 null mice display distinct pattern and time course of cellular degeneration in the cochlea. *J Comp Neurol*. 2009; 516:569–579. [PubMed: 19673007]
22. Chang Q, Tang W, Ahmad S, Zhou B, Lin X. Gap junction mediated intercellular metabolite transfer in the cochlea is compromised in connexin30 null mice. *PLoS ONE*. 2008; 3(12):e4088. [PubMed: 19116647]
23. Sun J, Ahmad S, Chen S, Tang W, Zhang Y, Chen P, et al. Cochlear gap junctions coassembled from Cx26 and 30 show faster intercellular Ca²⁺ signaling than homomeric counterparts. *Am J Physiol Cell Physiol*. 2005; 288(3):C613–23. [PubMed: 15692151]
24. Kikuchi T, Kimura RS, Paul DL, Adams JC. Gap junctions in the rat cochlea: immunohistochemical and ultrastructural analysis. *Anat Embryol (Berl)*. 1995; 191(2):101–18. [PubMed: 7726389]
25. Kho ST, Pettis RM, Mhatre AN, Lalwani AK. Safety of adeno-associated virus as cochlear gene transfer vector: analysis of distant spread beyond injected cochleae. *Mol Ther*. 2000; 2(4):368–73. [PubMed: 11020352]
26. Ishimoto S, Kawamoto K, Kanzaki S, Raphael Y. Gene transfer into supporting cells of the organ of Corti. *Hear Res*. 2002; 173(1-2):187–97. [PubMed: 12372646]
27. Pietola L, Aarnisalo AA, Joensuu J, Pellinen R, Wahlfors J, Jero J. HOX-GFP and WOX-GFP lentivirus vectors for inner ear gene transfer. *Acta Otolaryngol*. 2008; 128(6):613–20. [PubMed: 18568493]
28. Kawamoto K, Oh SH, Kanzaki S, Brown N, Raphael Y. The functional and structural outcome of inner ear gene transfer via the vestibular and cochlear fluids in mice. *Mol Ther*. 2001; 4(6):575–85. [PubMed: 11735342]
29. Iizuka T, Kanzaki S, Mochizuki H, Inoshita A, Narui Y, Furukawa M, et al. Noninvasive in vivo delivery of transgene via adeno-associated virus into supporting cells of the neonatal mouse cochlea. *Hum Gene Ther*. 2008; 19(4):384–90. [PubMed: 18439125]
30. Lalwani AK, Walsh BJ, Reilly PG, Muzyczka N, Mhatre AN. Development of in vivo gene therapy for hearing disorders: introduction of adeno-associated virus into the cochlea of the guinea pig. *Gene Ther*. 1996; 3(7):588–92. [PubMed: 8818645]

31. Han JJ, Mhatre AN, Wareing M, Pettis R, Gao WQ, Zufferey RN, et al. Transgene expression in the guinea pig cochlea mediated by a lentivirus-derived gene transfer vector. *Hum Gene Ther.* 1999; 10(11):1867–73. [PubMed: 10446926]
32. Henckaerts E, Linden RM. Adeno-associated virus: a key to the human genome? *Future Virol.* 2010; 5(5):555–574. [PubMed: 21212830]
33. Akil O, Seal RP, Burke K, Wang C, Alemi A, Daring M, et al. Restoration of Hearing in the VGLUT3 Knockout Mouse Using Virally Mediated Gene Therapy. *Neuron.* 2012; 75(2):283–93. [PubMed: 22841313]
34. Qu Y, Tang WX, Zhou BF, Ahmad S, Chang Q, Li XM, et al. Early developmental expression of connexin26 in the cochlea contributes to its dominate functional role in the cochlear gap junctions. *Biochem and Biophys Res Commun.* 2011; 417(1):245–250. [PubMed: 22142852]
35. Bedrosian JC, Gratton MA, Brigande JV, Tang W, Landau J, Bennett J. In vivo delivery of recombinant viruses to the fetal murine cochlea: transduction characteristics and long-term effects on auditory function. *Mol Ther.* 2006; 14(3):328–35. [PubMed: 16765094]
36. Gubbels SP, Woessner DW, Mitchell JC, Ricci AJ, Brigande JV. Functional auditory hair cells produced in the mammalian cochlea by in utero gene transfer. *Nature.* 2008; 455(7212):537–41. [PubMed: 18754012]
37. Miwa T, Minoda R, Ise M, Yamada T, Yumoto E. Mouse Otocyst Transuterine Gene Transfer Restores Hearing in Mice With Connexin 30 Deletion-associated Hearing Loss. *Mol Ther.* 2013
38. Grimm D, Kay MA, Kleinschmidt JA. Helper virus-free, optically controllable, and two-plasmid-based production of adeno-associated virus vectors of serotypes 1 to 6. *Mol Ther.* 2003; 7(6):839–50. [PubMed: 12788658]
39. Grieger JC, Choi VW, Samulski RJ. Production and characterization of adeno-associated viral vectors. *Nature protocols.* 2006; 1(3):1412–28. [PubMed: 17406430]
40. Aurnhammer C, Haase M, Muether N, Hausl M, Rauschhuber C, Huber I, et al. Universal real-time PCR for the detection and quantification of adeno-associated virus serotype 2-derived inverted terminal repeat sequences. *Hum Gene Ther Methods.* 2012; 23(1):18–28. [PubMed: 22428977]
41. Ahmad, S.; Tang, W.; Chang, Q.; Qu, Y.; Hibshman, J.; Li, Y., et al. Restoration of connexin26 protein level in the cochlea completely rescues hearing in a mouse model of human connexin30-linked deafness. *Proceedings of the National Academy of Sciences of the United States of America*; 2007; p. 1337-41.
42. Thompson DC, McPhillips H, Davis RL, Lieu TL, Homer CJ, Helfand M. Universal newborn hearing screening: summary of evidence. *JAMA.* 2001; 286(16):2000–10. [PubMed: 11667937]

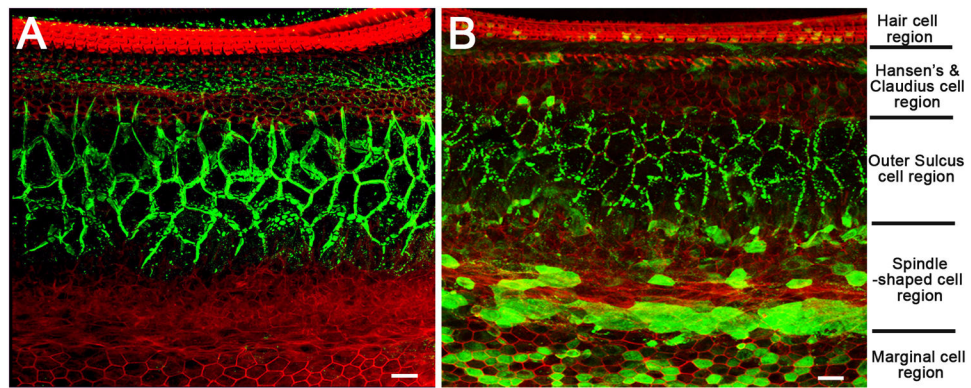


Figure 1. Comparison of endogenous and virally-mediated exogenous Cx26 expression in the cochlea

A) A confocal image showing the immunolabeling pattern of Cx26 (in green) taken from a flattened cochlear preparation of WT mouse. Major cochlear cell type regions are labeled on the right side of the figure. B) A confocal image showing the immunolabeling pattern of GFP (in green) taken from a flattened cochlear preparation of cCx26KO mouse received virus injection. The GFP is fused to the Cx26 in the design of the viral vector in order to differentiate exogenous Cx26 from residual endogenous Cx26 protein in the cCx26KO mice. The red counter-labeling was obtained with phalloidin conjugated to Alexa568. Scale bars in both panels represent approximately 20 μm .

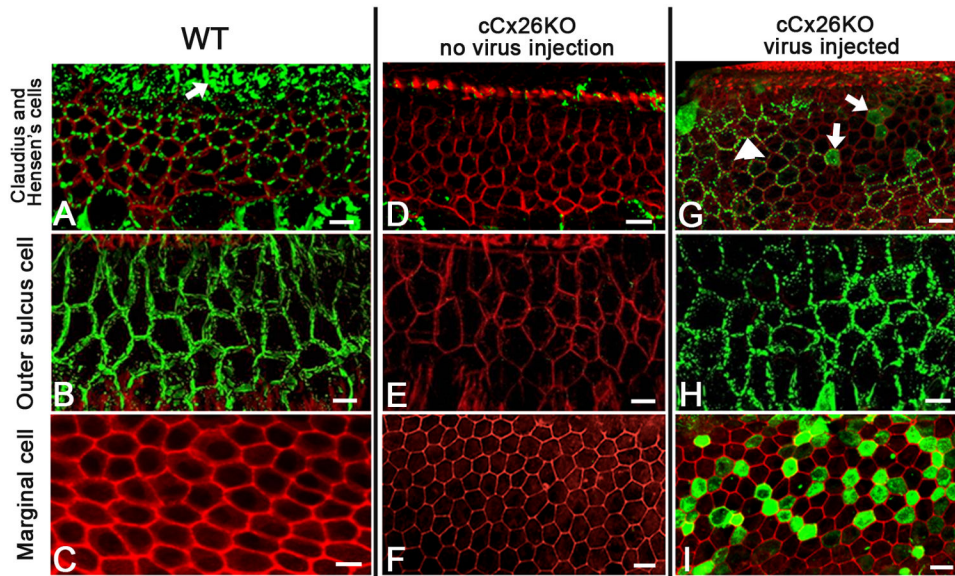


Figure 2. Detailed comparison of endogenous and virally-mediated exogenous Cx26 expression in cochlear cells

A-C): Confocal images showing the immunolabeling patterns of Cx26 (in green) taken from a flattened cochlear preparation of WT mouse in the Claudius cells (cell membrane outlined by the hexagonal red phalloidin counterstaining) and Hensen's cells (an example is indicated by an arrow) (A), outer sulcus cell (B) and marginal cells (C).

D-F) Confocal images showing the immunolabeling patterns of Cx26 (in green) taken from a flattened cochlear preparation of untreated cCx26KO mouse in the cochlear regions of Claudius cells (D), outer sulcus cell (E) and marginal cells (F).

G-I) Confocal images showing the immunolabeling results (in green) with an antibody against the GFP, demonstrating the distribution patterns of Cx26-GFP fusion protein in the cochlea of treated cCx26KO mouse in the cochlear regions of Claudius cells (D), outer sulcus cell (E) and marginal cells (F). The red counter-labeling was obtained with phalloidin conjugated to Alexa568. Scale bars in all panels represent approximately 50 μm .

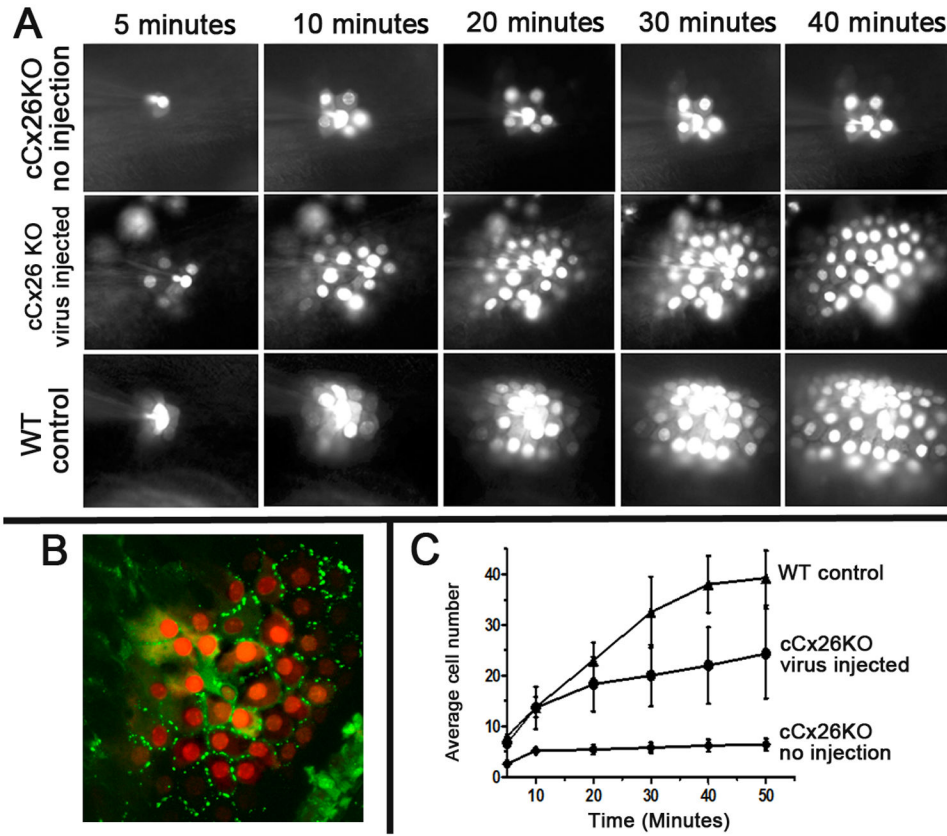


Figure 3. Result of dye diffusion assay used to evaluate the intercellular coupling among the cochlear outer sulcus cells of WT, treated and untreated cCx26KO mice

A) Time series images showing the diffusion of a charged fluorescent dye across GJs from one injected cells to neighboring cells. Results obtained from WT, treated and untreated cCx26KO mouse cochlea are given in the bottom row, middle row and top row, respectively.

B) GFP signal (green) overlapped with the dye (red) diffusion pattern, demonstrating that the cells are coupled by GJs. C) Quantification of the number of cells received the dye

diffusion among the outer sulcus cells over time in WT, treated and untreated cCx26KO mouse cochlea, as labeled in the figure.

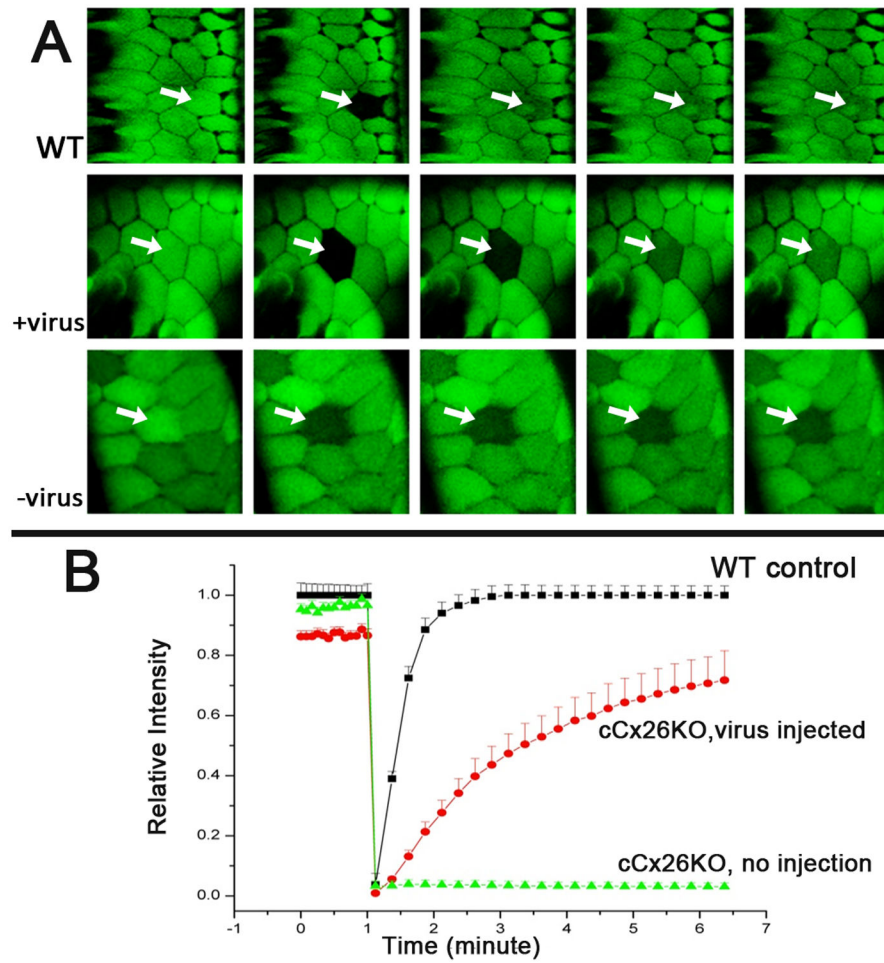


Figure 4. Results of FRAP assay for evaluating the intercellular coupling among the cochlear cells of WT, treated and untreated cCx26KO mice

A) Time series images showing the fluorescence recovery in the photo-bleached cells (indicated by white arrows) of WT (top row), treated (middle row) and untreated (bottom row) cCx26KO mouse cochlea. Time interval of each panel is one minute. The first panel shows the outer sulcus cells loaded with calcein AM just before photobleaching. The cell pointed by the white arrow was photobleached by intense laser light for 10 seconds, after which the fluorescence recovery in the cell is measured. B) Quantification of the FRAP results showing the relative fluorescence intensity change around the time when the cell is photobleached.

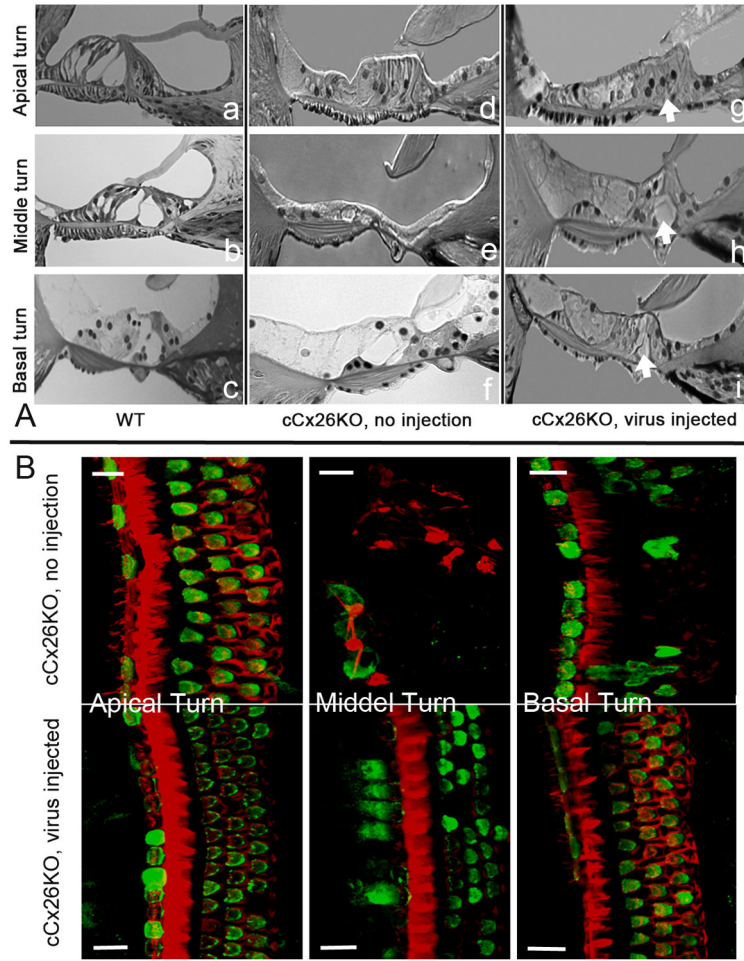


Figure 5. Morphological disease phenotypes in the organ of Corti of cCx26KO mouse cochlea were improved
 A) Images comparing the morphology of the organ of Corti in the WT (a-c), untreated (d-f) and treated (g-i) mice. Results obtained from the apical, middle and basal turns are given in the top, middle and bottom rows, respectively. B) Comparison of the hair cell (labeled green with an antibody against Myo6) survival in the cochlea of treated (bottom row) and untreated (top row) mice. Cochlear turns are labeled in the figure. The red counter-labeling was obtained with phalloidin conjugated to Alexa568. Scale bars in all panels represent approximately 50 μ m.

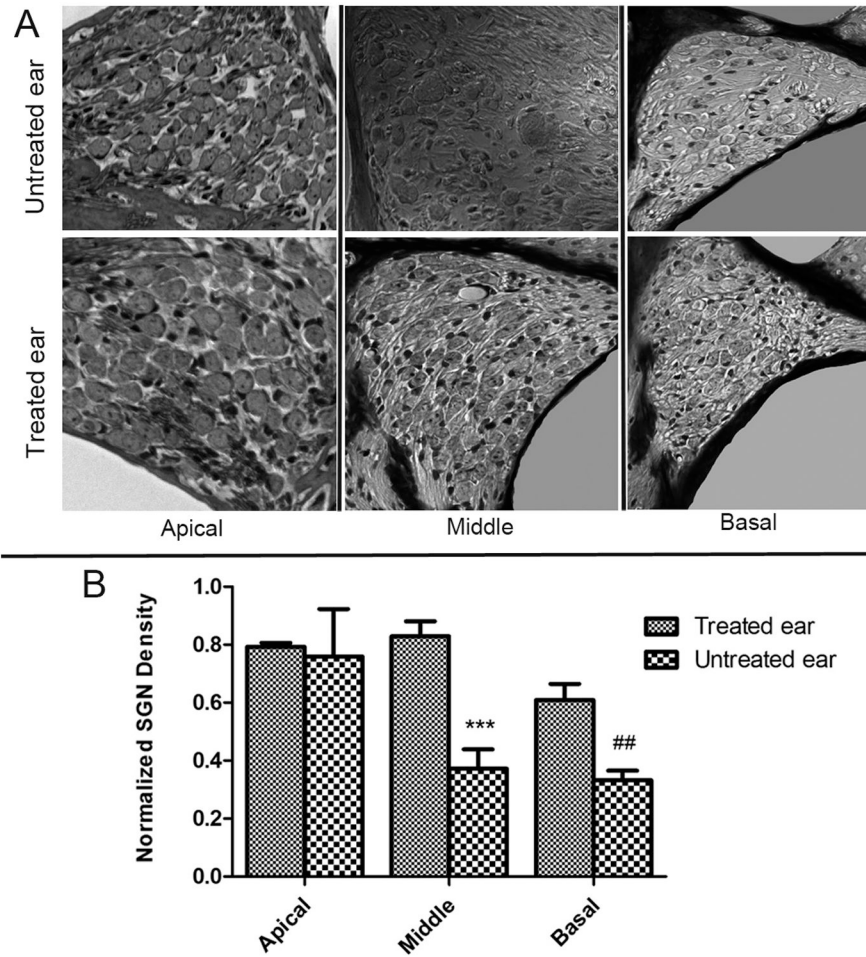


Figure 6. Secondary death of SG neuron after degeneration of the organ of Corti was significantly reduced in the treated cochlea of the middle and basal turns
 A) DIC images showing the SG neurons in cochlear sections of untreated (top row) and treated (bottom row) mice. B) Normalized SG neuron densities in the three cochlear turns are compared for the treated and untreated cochlea as labeled. Statistically significant differences between the two groups are denoted by symbols about the bars.

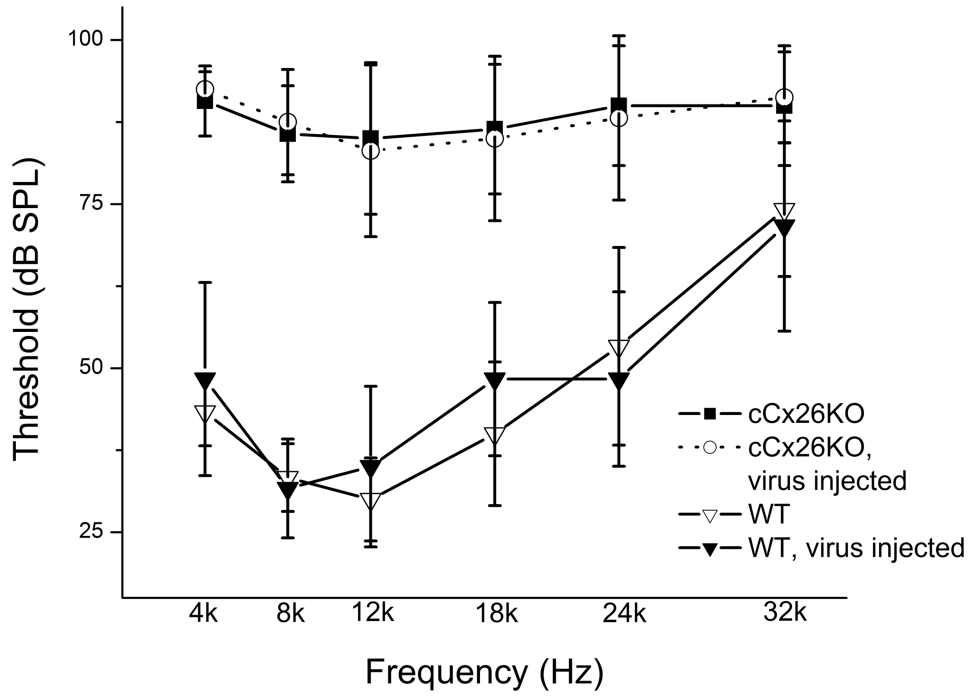


Figure 7. Tone-burst ABR test results of four groups of mice across a frequency range of 4k to 32 kHz. Hearing thresholds of WT and cCx26KO mice, either treated or untreated with virally-expressed Cx26 are given as labeled in the figure. The relatively high hearing thresholds at higher frequencies (e.g., 24-32 kHz) were caused by the acoustic property of the speaker and the tube connecting the speaker to the ear we used in experiments.

Transduction efficiency (% of cells transfected, n>100 in all cases) in various types of cochlear cells at different cochlear turns.

Table 1

| | Hair Cells | Hensen's cells | Claudius Cells | Outer Sulcus Cells | Spindle -Shaped cell | Marginal Cells |
|-------------|------------|----------------|----------------|--------------------|----------------------|----------------|
| Basal turn | 44±3 | 13±2 | 47±8 | 99±0.5 | 61±7 | 45±4 |
| Middle turn | 32±4 | 10±3 | 28±7 | 98±1 | 41±5 | 32±7 |
| Apical turn | 13±2 | 7±2 | 11±3 | 98±1 | 32±5 | 21±3 |